

Effect of Compactified Dimensions and Background Magnetic Fields on the Phase Structure of $SU(N)$ Gauge Theories

Massimo D'Elia^{*} and Marco Mariti[†]

INFN—Sezione di Pisa, Largo Pontecorvo 3, I-56127 Pisa, Italy and Dipartimento di Fisica dell'Università di Pisa, Largo Pontecorvo 3, I-56127 Pisa, Italy

(Received 30 December 2016; revised manuscript received 13 March 2017; published 24 April 2017)

We discuss the properties of non-Abelian gauge theories formulated on manifolds with compactified dimensions and in the presence of fermionic fields coupled to magnetic backgrounds. We show that different phases may emerge, corresponding to different realizations of center symmetry and translational invariance, depending on the compactification radius and on the magnitude of the magnetic field. Our discussion then focuses on the case of an $SU(3)$ gauge theory in four dimensions with fermions fields in the fundamental representation, for which we provide some exploratory numerical lattice results.

DOI: 10.1103/PhysRevLett.118.172001

In this study, we investigate a class of phenomena taking place in $SU(N)$ gauge theories with dynamical fermions, when one of the space-time dimensions is compactified in the presence of an electromagnetic background coupled to the fermions. Such phenomena result from the coupling of the gauge field holonomy to the background, through fermion loops, leading to an entanglement between center and translational symmetries, which manifests itself through the presence of different phases and phase transitions.

Center symmetry plays a fundamental role in determining the phase diagram of pure $SU(N)$ gauge theories [1]. Their action is symmetric under gauge transformations which are periodic in the compactified direction, apart from a constant element belonging to the center of the gauge group. In the lattice formulation, that can be rephrased in terms of multiplication of all gauge links pointing in the compactified direction and taken at a given slice orthogonal to it by a center element $Z_N \equiv \{e^{i2k\pi/N}, k = 0, \dots, N-1\}$. This symmetry can be exact or spontaneously broken; the trace of the holonomy along the compactified direction, $L \equiv \text{Tr} \exp(i \oint dx_\mu g A_\mu)$ (Wilson line or Polyakov loop), which gets multiplied by Z_N , is a possible order parameter. Its expectation value $\langle L \rangle$ becomes nonzero and proportional to a center element for small enough compactification radii, due to the appearance of N degenerate vacua in the holonomy effective potential. For a thermal compactification, the corresponding phase transition describes deconfinement [2].

The presence of matter fields changes the picture substantially. The covariant derivative in the fermion action introduces a coupling to the holonomy around the compactified direction, which breaks center symmetry explicitly. For fermions in the fundamental representation and thermal boundary conditions (b.c.), this coupling favors a real Wilson line, so that the spontaneous breaking disappears. (For periodic b.c., positive real values are instead

disfavored, and a spontaneous breaking of the residual center symmetry is still possible [3–5].) A more interesting phenomenology takes place when fermions are coupled to an additional $U(1)$ background; i.e., their covariant derivative is

$$D_\nu = \partial_\nu + igA_\nu^a T^a + iq a_\nu, \quad (1)$$

where T^a are the $SU(N)$ generators and q is the coupling to the external $U(1)$ field a_μ . A well-known example is that of an imaginary chemical potential, $\mu = i\mu_I$ in finite temperature QCD. In this case, $q a_\nu = \mu_I \delta_{\nu 0}$, where 0 is the Euclidean temporal direction, and the full holonomy entering the fermion determinant is

$$\text{Tr} \exp \left(\oint dx_\mu i(gA_\mu + qa_\mu) \right) = L e^{i\mu_I/T}. \quad (2)$$

It is therefore $L \exp(i\mu_I/T)$ which tends to be oriented along the real direction; i.e., in this case fermions tend to align L along $\exp(-i\mu_I/T)$, like an external field whose direction in the complex plane is fixed by μ_I/T . This is exemplified in Fig. 1 for the $SU(3)$ case. In the high- T phase, where the pure gauge contribution to the holonomy effective potential would tend to align it along a center

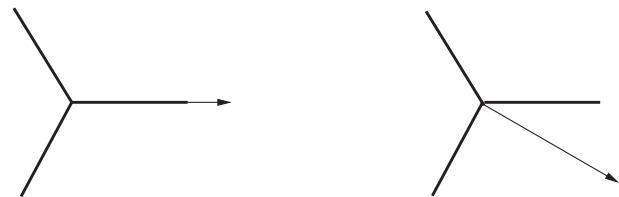


FIG. 1. Dynamical fermions break center symmetry like an external field in a spin system, e.g., a three-state Potts model for $SU(3)$. For standard thermal b.c., the external field points along the real axis (left), while the introduction of an imaginary chemical potential rotates it (right).

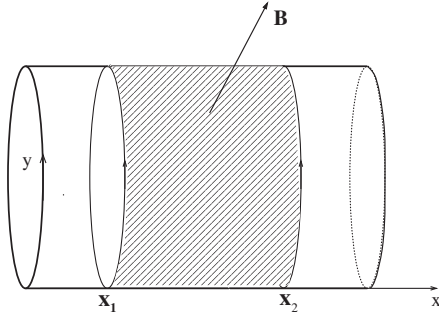


FIG. 2. Space dimension y is compactified in the presence of a background field. The non-Abelian holonomies sitting at x_1 and x_2 couple differently to dynamical fermions, depending on the flux of the field across the shaded surface.

element, that results in first-order phase transitions as μ_I/T crosses π/N or odd multiples of it, which are known as Roberge-Weiss transitions [6].

We are going to explore what happens when the $U(1)$ background is nonuniform. To fix ideas, we consider the case in which a spatial dimension gets compactified in the presence of a background magnetic field; notice however that the case of thermal b.c. in the compactified dimension is equivalent, since the antiperiodic b.c. for fermions imply just a global shift of the $U(1)$ gauge field. Moreover, we consider for simplicity the case in which all fermions have the same electric charge.

Let us consider the situation depicted in Fig. 2: Direction y is compactified in the presence of a magnetic field orthogonal to the $\mathbf{x} - \mathbf{y}$ plane. The Wilson line sitting at \mathbf{x}_1 couples to dynamical fermions of charge q through a local phase factor, i.e., in the combination $L(\mathbf{x})e^{iq \oint dy a_y(\mathbf{x}, y)} = L(\mathbf{x})e^{i\phi(\mathbf{x})}$: Such a coupling tends to align the Wilson line along the center element closest to $e^{-i\phi(\mathbf{x})}$. However, because of the \mathbf{x} dependence, it tends to align Wilson lines sitting at different values of the noncompactified coordinates along different center elements; i.e., the $U(1)$ background field may induce for small enough compactification length L_c , a structure of different center domains.

Whereas the value of a single phase factor is not physically relevant and gauge dependent, the phase difference between different points is. Indeed, we have

$$\begin{aligned} e^{i[\phi(\mathbf{x}_2) - \phi(\mathbf{x}_1)]} &= \exp\left(iq \oint dy [a_y(\mathbf{x}_2, y) - a_y(\mathbf{x}_1, y)]\right) \\ &= e^{iq\Phi_B}, \end{aligned} \quad (3)$$

where Φ_B is the total magnetic field flux going through the shadowed surface in Fig. 2. Despite the simplified situation, it is easy to realize that the value of this flux is, for any magnetic field distribution, a property of the points \mathbf{x}_1 and \mathbf{x}_2 only, independent of the shape of the surface in the noncompactified directions. Therefore, modulo a global center rotation, the structure of center domains that tends to be formed is a unique property of the magnetic background.

However, the fact that such a structure actually forms is nontrivial, since different center domains imply the presence of interfaces separating them, which has a cost in terms of energy. The actual structure will depend on the balance between the energy spent in creating center interfaces and the energy spent in keeping the holonomy in a locally wrong vacuum: The former is a function of the interface tension and of the density of interfaces, which depends on the magnetic field strength, and the latter is a function of the holonomy effective potential. Since both the interface tension and the effective potential are functions of L_c , one may expect that different phases, corresponding to different center domain structures, are crossed as the compactification radius shrinks, with corresponding phase transitions and metastable states.

To facilitate the discussion, let us focus on a four-dimensional (4D) gauge theory with a uniform and constant magnetic background field $F_{xy} = B$. We will compare two extreme situations: that in which all center domains are actually formed (i.e., the holonomy is in the correct “local vacuum” everywhere) and that in which the holonomy stays in the same center sector everywhere, without forming any interface. In the first case, making reference to Fig. 2, the number of interfaces, N_{int} , is given by the different center sectors spanned by the local phase between x_1 and x_2 , i.e.,

$$N_{\text{int}} = q\Phi_B / (2\pi/N) = qBL_c N / 2\pi, \quad (4)$$

where $L = |x_2 - x_1|$, while in the second case one must keep the holonomy in the wrong center sector for a fraction $(N - 1)/N$ of the region between x_1 and x_2 .

In the small L_c limit, we can recover perturbative results obtained in the thermal field theory, where Euclidean time is compactified and $T = 1/L_c$. The interface tension (i.e., the energy per unit interface area) is proportional to $L_c^{-3} \log(1/L_c)$ [7], and the energy density spent to keep the holonomy in the wrong vacuum is proportional to L_c^{-4} [6]. Apart from a common integration factor over the noncompactified directions orthogonal to x , the energy spent to create all possible interfaces between x_1 and x_2 is then proportional to $qBL_c^{-2} \log(1/L_c)$, while the energy spent to maintain the holonomy in the same center sector, without creating any interface, is proportional to LL_c^{-4} . The first situation is clearly favored, at a fixed magnetic field, for small enough L_c and, at fixed L_c , for small enough B . For intermediate values of L_c and/or B , the lowest energy configuration might correspond to a partial formation of the center domain structure, so that various phase transitions can be crossed as the two quantities change. Given the power law dependence on L_c , a similar behavior is expected when L_c is changed at fixed total flux, i.e., if $B \propto 1/L_c$.

Note that, for a uniform background, an exact symmetry appears: An elementary center transformation can be reabsorbed by a translation along x by $2\pi/(qBL_c N)$. This discrete symmetry can be either exactly realized or spontaneously broken. In the first case, after each

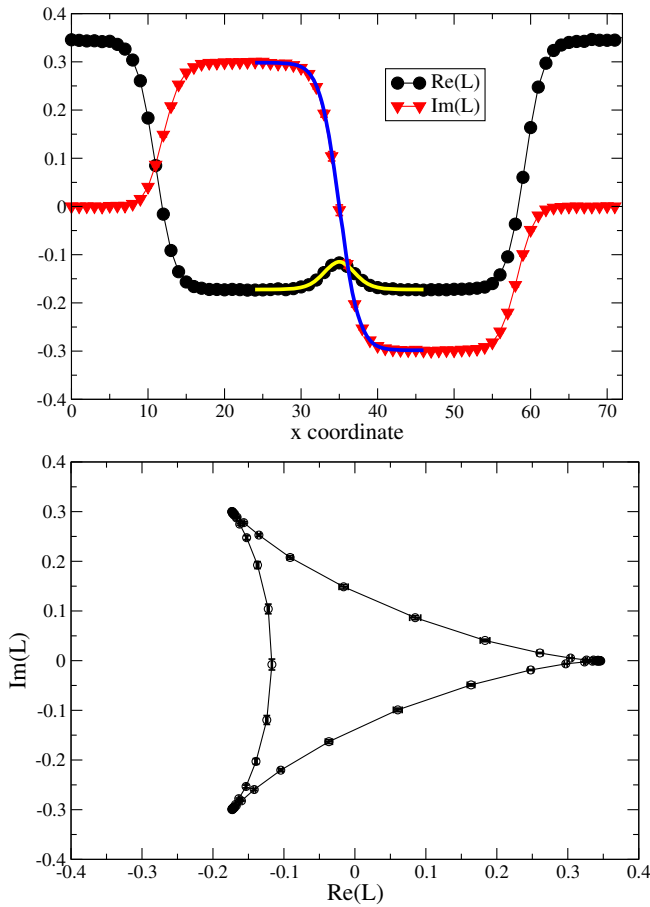


FIG. 3. Local average of the real and imaginary parts of the Wilson line as a function of x (up) and in the complex plane (down), for $L_x = 72$, $L_c = 4$, and $b = 1$ [see Eq. (7)]. Thick lines in the upper figure represent a fit to the perturbative interface profile [7,16–18].

translation by $2\pi/(qBL_cN)$ the holonomy rotates by $-2\pi/N$, and the spatial average of the Wilson line is exactly zero. In the second case, the holonomy fails to rotate and stays in a false vacuum somewhere. Therefore, the spatial average of the Wilson line could be nonzero and may serve as a nonlocal order parameter. We notice an analogy with the topological order parameter of Ref. [8], where the imaginary quark density is integrated over a loop in the complex chemical potential and keeps a trace of center domain crossings during the loop.

Numerical simulations.—To test this scenario, we have performed numerical simulations of a 4D $SU(3)$ gauge theory, with two degenerate and equally charged dynamical flavors in the fundamental representation, adopting the rational hybrid Monte Carlo algorithm [9] implemented on Graphics Processing Units (GPUs) [10]. The theory has been discretized with standard rooted staggered fermions on a periodic 4D torus, with a uniform magnetic field orthogonal to the $x - y$ plane and the y direction significantly shorter than the others, as in Fig. 2. The partition function reads

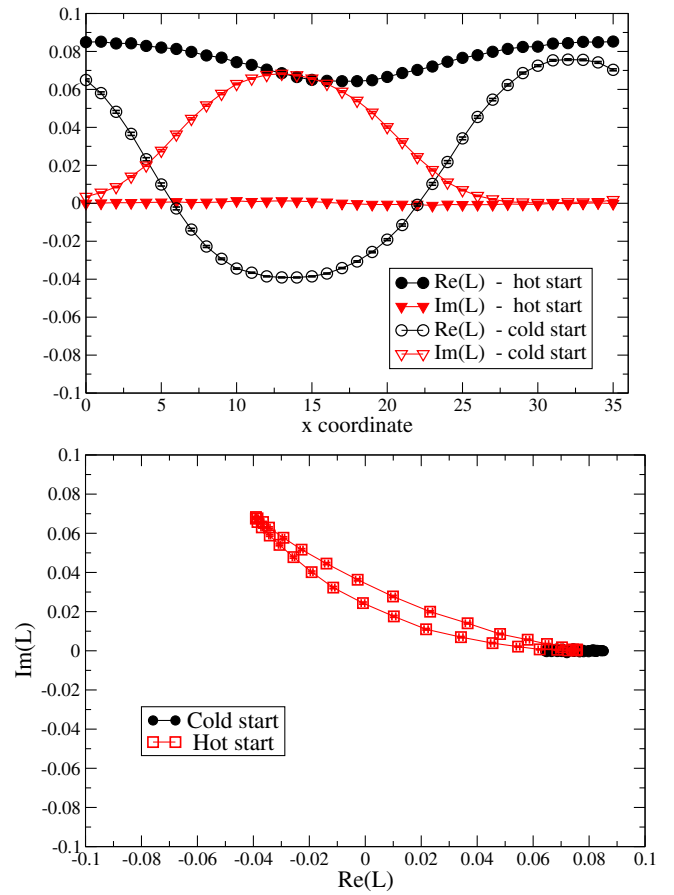


FIG. 4. As in Fig. 3, for $L_x = 36$, $L_c = 8$, $b = 1$ (corresponding to the same B of Fig. 3), and two different simulations, starting from random (hot) or unit (cold) gauge links. In both cases, the center-translational symmetry is spontaneously broken: For the cold start a single center domain is formed, and for the other a phase with two center domains emerges.

$$Z \equiv \int \mathcal{D}U e^{-S_G} \det D^{1/2}[U, q], \quad (5)$$

$$D_{i,j}^{(q)} \equiv am\delta_{i,j} + \frac{1}{2} \sum_{\nu=1}^4 \eta_{\nu}(i) [u_{\nu}^{(q)}(i) U_{\nu}(i) \delta_{i,j-\hat{\nu}} - u_{\nu}^{*(q)}(i-\hat{\nu}) U_{\nu}^{\dagger}(i-\hat{\nu}) \delta_{i,j+\hat{\nu}}], \quad (6)$$

where $\mathcal{D}U$ is the integration over $SU(3)$ gauge links, S_G is the plaquette pure gauge action, i and j are lattice site indexes, and $\eta_{\nu}(i)$ are staggered phases. The $U(1)$ phases $u_{\mu}^{(q)}(i)$ are chosen to reproduce a uniform magnetic field across the $x - y$ plane, which, as a consequence of the periodic b.c., is quantized according to [11–14]

$$qB = 2\pi b/(L_x L_y a^2), \quad (7)$$

where b is an integer. The number of different center sectors which should be crossed when moving along the x direction is then equal to $Nb = 3b$.

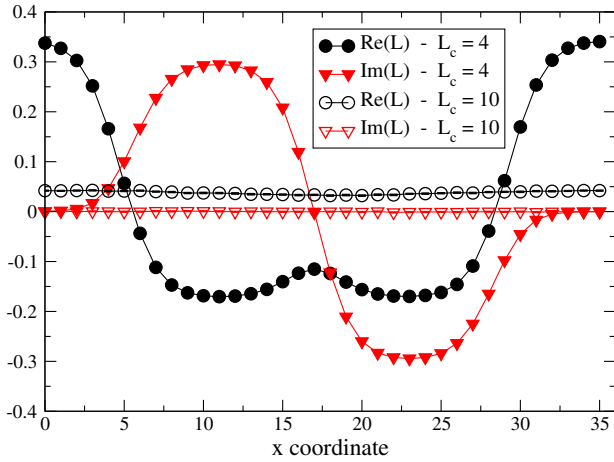


FIG. 5. Local average of the real and imaginary parts of the Wilson line for $L_x = 36$ and $L_c = 4, 10$, keeping the total magnetic flux unchanged ($b = 1$).

We have worked in a fixed cutoff scheme, setting the inverse gauge coupling $\beta = 6/g_0^2 = 6.2$ and the bare quark mass $am = 0.01$ in all simulations. We have considered $L_x \times L_y \times L_z \times L_t$ lattices, fixing $L_x = L_t = 24$ and then tuning $L_y = L_c$ to change the compactification radius and L_x and b to change the magnetic background at fixed L_c . Such bare values correspond roughly to a pion mass of the order of the ρ mass [15]. For all explored values of the compactification radius, the corresponding thermal system at a zero background field is in the deconfined phase.

In Fig. 3, we show results for the real and imaginary parts of the Wilson line from simulations with $L_y = 4$, $L_x = 72$, and $b = 1$; data are reported both as a function of x and in the complex plane. The center-translational symmetry is realized exactly: The predicted three center domains, separated by three interfaces, are clearly visible, and the system is globally center symmetric. We notice that the interface (domain wall) profiles are nicely described by the functional form predicted by the perturbation theory [7,16–18]: A fit to such a prediction [see, e.g., Eq. (22) of Ref. [18]] is reported in Fig. 3.

However, as we increase L_c while keeping $B \propto b/(L_c L_x)$ fixed, the situation changes. In Fig. 4, we report results obtained for $L_c = 8$. In this case, two different phases emerge, depending on the starting configuration of the simulation. In both of them, the global center symmetry is spontaneously broken: In one phase, the system chooses a single center domain, as for a standard thermal system in the high- T regime; therefore, we name it the “deconfined phase”; in the other, instead two center domains are formed, with the corresponding separating interfaces and, due to the characteristic shape in the complex plane (see Fig. 4), we name it the “banana phase.” For $L_c = 6$ one finds that the global center symmetry is exact, while for $L_c > 8$ only the deconfined phase survives. The metastability found for

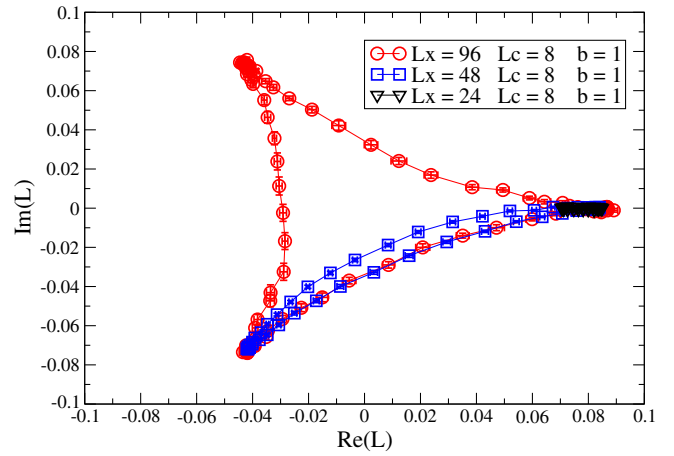


FIG. 6. Local average of the real and imaginary parts of the Wilson line in the complex plane, for $L_c = 8$ and three values of B , for which three different phases are found.

$L_c = 8$ is a clear suggestion that the different phases are separated by strong first-order transitions.

A similar pattern takes place if one changes L_c at a fixed magnetic flux, i.e., by scaling $B \propto 1/L_c$. This is visible in Fig. 5, showing two different compactifications $L_c = 4$ and 10 , with the same flux as for the $L_c = 8$ case in Fig. 4.

Finally, in Fig. 6, we show a set of results in which B is changed at fixed L_c . As expected, as B increases, the system moves from the phase with an exact global center symmetry to the banana phase and, finally, to the deconfined phase; in all examples shown the phases are stable; i.e., they are found independently of the starting configuration.

A nonlocal order parameter for the realization of the center-translational symmetry is the spatial average of the Wilson line over all noncompactified directions. Its time history is reported in Fig. 7 for some of the cases discussed above, including the metastable case reported in Fig. 4.

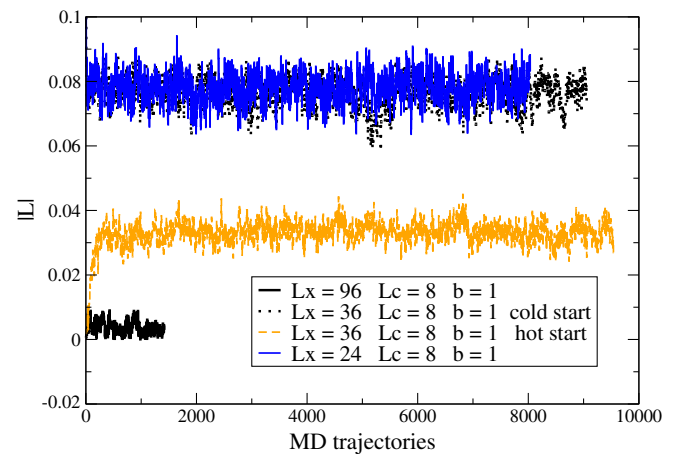


FIG. 7. Monte Carlo histories of the modulus of the spatially averaged Wilson line (order parameter for center-translational symmetry) for simulations at fixed L_c and variable B .

Concluding remarks.—We have discussed how the compactification of a non-Abelian gauge theory in the presence of a $U(1)$ background field is accompanied by the formation of a structure of center domains, dictated by the dynamics of the holonomy, for asymptotically small values of L_c . As L_c increases, the energetically favorable structure can change, leading to different phases characterized by a reduced number of domains; such phases are likely separated by first-order transitions, leading to the formation of metastable states. A similar behavior is found as B increases at fixed L_c .

We have focused on $SU(3)$ with degenerate fermions. If the electric charges are different and/or for different gauge groups, the structure of center domains can be different because of the competing contributions from differently charged fermions. However, the general picture will be similar and will not be changed even in the presence of a different number of noncompactified dimensions.

Therefore, our results, in particular, the appearance of different phases and of metastable states and domain walls as L_c and/or B change, could be of interest for various contexts, like for gauge theories with extra dimensions which get compactified in the presence of background fields but possibly also for condensed matter systems presenting an emerging non-Abelian symmetry.

We thank Claudio Bonati, Michele Mesiti, and Francesco Negro for very useful discussions. Numerical simulations have been performed on a GPU farm located at the INFN Computer Center in Pisa and on the QUONG cluster in Rome.

*massimo.delia@unipi.it

†marco.mariti@df.unipi.it

- [1] G. 't Hooft, *Nucl. Phys.* **B138**, 1 (1978).
- [2] B. Svetitsky and L. G. Yaffe, *Nucl. Phys.* **B210**, 423 (1982).
- [3] T. DeGrand and R. Hoffmann, *J. High Energy Phys.* **02** (2007) 022.
- [4] B. Lucini, A. Patella, and C. Pica, *Phys. Rev. D* **75**, 121701 (2007).
- [5] M. D'Elia and F. Sanfilippo, *Phys. Rev. D* **80**, 111501 (2009).
- [6] A. Roberge and N. Weiss, *Nucl. Phys.* **B275**, 734 (1986).
- [7] T. Bhattacharya, A. Gocksch, C.K. Altes, and R.D. Pisarski, *Phys. Rev. Lett.* **66**, 998 (1991); *Nucl. Phys.* **B383**, 497 (1992).
- [8] K. Kashiwa and A. Ohnishi, *Phys. Rev. D* **93**, 116002 (2016).
- [9] M. A. Clark and A. D. Kennedy, *Nucl. Phys. B, Proc. Suppl.* **129–130**, 850 (2004); *Phys. Rev. Lett.* **98**, 051601 (2007).
- [10] C. Bonati, G. Cossu, M. D'Elia, and P. Incardona, *Comput. Phys. Commun.* **183**, 853 (2012).
- [11] G. 't Hooft, *Nucl. Phys.* **B153**, 141 (1979).
- [12] J. Smit and J. C. Vink, *Nucl. Phys.* **B286**, 485 (1987).
- [13] P. H. Damgaard and U. M. Heller, *Nucl. Phys.* **B309**, 625 (1988).
- [14] M. H. Al-Hashimi and U. J. Wiese, *Ann. Phys. (N.Y.)* **324**, 343 (2009).
- [15] T. Blum, L. Karkkainen, D. Toussaint, and S. A. Gottlieb, *Phys. Rev. D* **51**, 5153 (1995).
- [16] C. Korthals Altes, A. Michels, M. A. Stephanov, and M. Teper, *Phys. Rev. D* **55**, 1047 (1997).
- [17] P. Giovannangeli and C. P. Korthals Altes, *Nucl. Phys.* **B608**, 203 (2001).
- [18] F. Bursa and M. Teper, *J. High Energy Phys.* **08** (2005) 060.